Two-Dimensional Spatially-Selective RF Excitation Pulses in Echo-Planar Imaging

Susanne Rieseberg, Jens Frahm, and Jürgen Finsterbusch*

Two-dimensional spatially-selective RF (2DRF) excitation pulses were developed for single-shot echo-planar imaging (EPI) with reduced field of view (FOV) in the phase-encoding direction. The decreased number of *k*-space lines significantly shortens the length of the EPI echo train. Thus, both gradient-echo and spin-echo 2DRF-EPI images of the human brain at 2.0 T exhibit markedly reduced susceptibility artifacts in regions close to major air cavities. Based on a blipped-planar trajectory, implementation of a typical 2DRF pulse resulted in a 26-ms pulse duration, a 5-mm section thickness, a 40-mm FOV along the phase-encoding direction, and a 200-mm distance of the unavoidable side excitations from the center of the FOV. For the above conditions and at 2 × 2 mm^2 resolution, 2DRF-EPI yielded an echo train length of only 21 ms, as opposed to 102 ms for conventional EPI. This gain in time may be used to achieve higher spatial resolution. For example, spin-echo 2DRF-EPI of a 40-mm FOV at 1 × 1 mm^2 resolution led to an echo train of 66 ms. Although the current implementation still lacks user-friendliness, 2DRF pulses are likely to become a useful addition to the arsenal of advanced MRI tools. Magn Reson Med 47:1186–1193, 2002. © 2002 Wiley-Liss, Inc.

Key words: magnetic resonance imaging; zoom imaging; localized imaging; 2D-selective RF excitation; echo-planar imaging

Echo-planar imaging (EPI) and spiral imaging are single-shot MRI techniques based on the rapid acquisition of a train of sign-alternating gradient echoes (1,2). They offer high signal-to-noise ratios (SNRs) and imaging speed (volume coverage) which render them attractive for functional neuroimaging and diffusion-weighted MRI. However, applications of EPI and spiral imaging may be hampered by inherent problems, such as ghosting or ringing artifacts, as well as by geometric distortions and signal losses caused by chemical shift and susceptibility differences. These effects degrade the achievable image quality and limit the spatial resolution. In physical terms, the artifacts reflect signal phase distortions that accumulate with increasing gradient echo time and mimic the encoding of spatial information during image reconstruction. While various strategies have been proposed to alleviate this well-known problem, the fundamental solution for overcoming these limitations is the use of shorter echo trains.

There are several possible means of minimizing these artifacts. Whereas a simple reduction of the number of gradient echoes would sacrifice the spatial resolution or cause image aliasing, the use of faster gradient switching is limited by the occurrence of physiological nerve stimulation. A successful solution is the use of *k*-space segmentation of the image data in a multishot acquisition (3,4). However, this idea not only prolongs the imaging time but may also lead to shot-to-shot phase variations, to which some methods, such as diffusion-weighted MRI, are sensitive. Another promising development has emerged from an adaptation of parallel imaging techniques based on multiple receiver coils with simultaneous acquisition of spatial harmonics (SMASH) (5); sensitivity-encoding (SENSE) (6); or partially parallel imaging with localized sensitivities (PILS) (7), which in preliminary applications led to beneficial effects for single-shot EPI (8). Nevertheless, the achievable echo-train reduction seems to be limited to a factor of 2–4, which may still lead to echo trains that are too long to adequately deal with the enhanced susceptibility problems at field strengths of 3 T or higher.

A complementary way of decreasing the echo train is to reduce the field of view (FOV) along the phase-encoding dimension of the image while simultaneously avoiding image aliasing. First attempts used spin-echo and stimulated-echo EPI sequences with orthogonal RF pulses to excite an inner FOV and thereby reduce the number of *k*-space lines required for image reconstruction (9,10). A major drawback of these techniques is the restricted volume coverage due to neighboring sections becoming presaturated by one of the RF excitations. Furthermore, the sequences acquire RF refocused echoes, and therefore are not generally applicable to functional neuroimaging commonly based on gradient-echo EPI.

The purpose of the present work was to combine 2D spatially selective RF (2DRF) excitation pulses with single-shot EPI for human brain applications. The approach allows for (1) reduced FOV imaging with correspondingly shorter echo trains, (2) gradient-echo versions for functional neuroimaging, and (3) access to unrestricted volume coverage by successive multislice imaging. Whereas a previous study combined 2DRF excitation with EPI to reduce the imaging time of segmented 3D-EPI for coronary MR angiography (MRA) (11), the main goal of this work was to assess the gains in image quality of single-shot EPI that result from either reduced susceptibility artifacts in the vicinity of air-tissue boundaries or from higher spatial resolution.

Although multidimensional spatially-selective RF excitations were theoretically described and experimentally realized more than a decade ago (12), their practical implementation has only recently been facilitated by considerable advances in gradient hardware initiated by the increasing demand for high-speed MRI. 2DRF pulses have been exploited particularly for the visualization of myocardial wall motion with high temporal resolution (13), and to achieve flow-sensitivity in two dimensions in time-

Biomedizinische NMR Forschungs GmbH am Max-Planck-Institut für biophysikalische Chemie, Göttingen, Germany.

*Correspondence to: Jürgen Finsterbusch, Ph.D., Biomedizinische NMR Forschungs GmbH, 37070 Göttingen, Germany. E-mail: jfinste@gwdg.de

Received 5 November 2001; revised 18 January 2002; accepted 24 January 2002.

DOI 10.1002/mrm.10157

Published online in Wiley InterScience (www.interscience.wiley.com).

of-flight angiography (14). Further applications allow for curved sections (15) and provide T_2^* contrast in line scan imaging (16).

MATERIALS AND METHODS

All studies were carried out on a 2.0 T Siemens Magnetom Vision (Siemens Medical Systems, Erlangen, Germany) with a 25 mT m^{-1} gradient system and a standard head coil. Whereas EPI data acquisition was based on the maximum available slew rate of 160 T m^{-1} s^{-1}, the gradient waveforms for 2DRF excitation were limited to a slew rate of 40 T m^{-1} s^{-1} to ensure their general applicability in sequences other than EPI. The calculation of 2DRF waveforms was accomplished using an algorithm developed by Thomas Kluge (Siemens Medical Systems) (17). It delivers the required RF pulse shape or $B_1(t)$ field strength for a given excitation volume (in two dimensions) and desired gradient trajectory. Written informed consent was obtained from all subjects prior to the examination.

Theoretical Framework

This section briefly summarizes the K-space formalism developed by Pauly et al. (12). In particular, it defines the relationship between the RF pulse shape and the 2D excitation volume, which significantly facilitates the comprehension of the actual 2DRF pulse design. Although the method neglects relaxation and resonance offset effects and represents an approximation for low flip angles, it has been shown to be reasonably useful for flip angles as high as 90° (12).

Considering a selective RF excitation between t_0 and t_1 with a time-dependent gradient field $\mathbf{G}(t)$ and the gyromagnetic ratio γ

$$\mathbf{K}(t) = -\gamma \int_t^{t_1} \mathbf{G}(t')dt' \qquad t_0 \le t \le t_1 \qquad [1]$$

represents the 1D trajectory in the 3D K-space.

The dimensionless excitation profile $P(\mathbf{r})$ defines the relative amount of longitudinal magnetization flipped into the transverse plane by the RF excitation, i.e., the ratio of the transverse magnetization after the RF excitation and the original longitudinal magnetization. In terms of $\mathbf{G}(t)$ and the RF field $B_1(t)$

$$P(\mathbf{r}) = F(W(\mathbf{K}) \cdot S(\mathbf{K})) = F(W(\mathbf{K})) * F(S(\mathbf{K})) \qquad [2]$$

where F denotes the Fourier transformation (FT), $*$ the convolution,

$$W(\mathbf{K}(t)) = \left(i\frac{B_1(t)}{|\mathbf{G}(t)|} \right)_{t=t(\mathbf{K})} \qquad [3]$$

the so-called weighting function, i.e. the B_1 field along the trajectory as a function of $\mathbf{K}$ instead of t, and $S(\mathbf{K})$ the sampling function with $S(\mathbf{K}) = 1$ for values of k that are part of the trajectory as given in Eq. [1], and $S(\mathbf{K}) = 0$ elsewhere. If $S(\mathbf{K}) = 1$ for all $\mathbf{K}$, the excitation profile is given by the FT of the weighting function, or conversely, in order to obtain a desired RF excitation volume, $W(\mathbf{K})$ should be chosen to be its FT.

The practical implementation of a 2DRF pulse is determined by additional factors, such as the restricted coverage of only a small region of the infinite K-space and the discrete nature of the sampling process. Finite extensions in K-space cause truncation effects and introduce blurring and ringing of the 2D excitation profile, in accordance with Eq. [2]. The ringing artifacts are commonly reduced by smoothing, e.g., with use of a Hanning or Gaussian filter function, which further increases blurring. Sampling of the 2D K-space is accomplished with a (gradient) trajectory that represents a 1D line. Thus, because $S(\mathbf{K})$ consists of discrete lines, the FT of the convolution in Eq. [2] leads to a central excitation volume at the desired position as well as periodic side excitations along the axes of discrete sampling. For example, whereas a spiral trajectory gives rise to circular side excitations, a blipped-planar trajectory as used here restricts side excitations to the direction of the "blip" gradient. In accordance with the properties of the FT, the distance of the side excitations increases with the sampling density.

Practical Design of 2DRF Pulses

Based on the above theory, and in view of foreseeable applications in neuroimaging, the practical design of a 2DRF pulse for EPI with a reduced FOV was guided by several boundary conditions. First, the pulse duration was limited to 26 ms. This served as a compromise between 2DRF performance, i.e., quality of the excitation profile, and the necessity to avoid pronounced relaxation effects during RF excitation and, more importantly, excessive T_2^*-weighting in gradient-echo 2DRF-EPI. Second, the spatial dimensions of the 2DRF pulse were targeted to excite a volume of 40 mm in the FOV direction (K_y) with 5-mm section thickness (K_x). These parameters allow for adequate single-shot coverage of various brain systems, including the primary motor cortex, visual cortex, auditory cortex, amygdala, and spinal cord.

As demonstrated in Fig. 1, the predefined excitation profile emerges as a rectangular stick (Fig. 1a). The corresponding weighting function obtained by FT yields a 2D sinc function in which the width in the direction of the slice is much broader than in the direction of the reduced FOV (Fig. 1b). To allow for maximum flexibility of the 2DRF pulse, the chosen K-space trajectory was based on a blipped-planar trajectory (Fig. 1c). It limits the unavoidable side excitations to a single direction. With a minimum distance of 200 mm from the center of the desired FOV, the side excitations could be shifted to regions outside the head for all orientations and even for the worst case of an FOV close to the skull, e.g., when measuring the visual cortex in a sagittal orientation.

The described requirements present stringent conditions. The large distance of the side excitations corresponds to a dense K-space sampling. This factor limits the achievable K-space coverage for the given 2DRF pulse duration and leads to a blurred excitation profile according to Eq. [2]. While blurring in the direction of the reduced FOV was compensated for by phase-encoding oversam-

pling, the slice profile was improved by a K-space range about fourfold larger in the slice direction (K_x) than in the direction of the reduced FOV (K_y). Accordingly, the orientation of the gradient trajectory line was assigned to the slice direction and the blip gradient to the FOV direction (Fig. 1c). To compensate for the 10-mm broad transition zones of the excitation profile in the FOV direction, the excitation volume (Fig. 1a) was set to 50 mm to achieve a central 40-mm plateau.

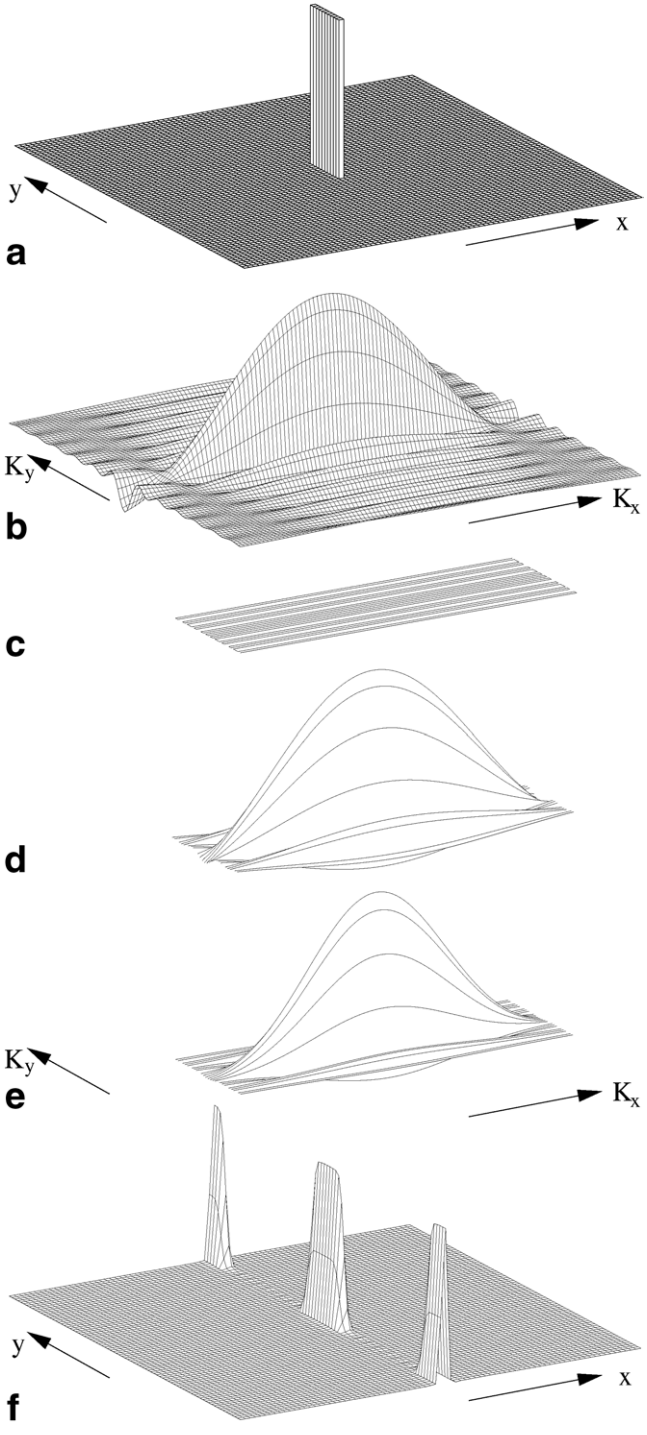

FIG. 1. Design of a 2DRF excitation pulse: (**a**) desired excitation profile, (**b**) weighting function obtained by FT of **a**, (**c**) choice of an appropriate blipped-planar K-space trajectory, (**d**) correspondingly sampled weighting function, (**e**) Gaussian filtering of the weighting function, and (**f**) excitation profile obtained by inverse FT of **e**. In comparison with **a**, the profile in **e** exhibits blurring and side excitations due to the discrete sampling of only a finite region in K-space.

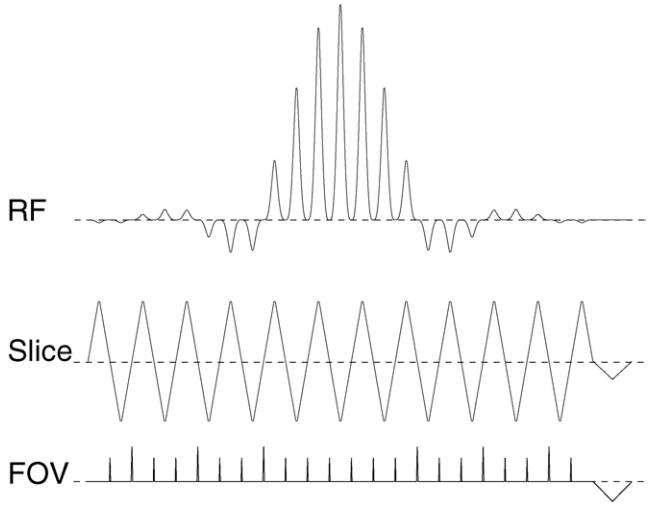

FIG. 2. Time courses of the B_1 field strength (RF) and two perpendicular gradients (slice, FOV) for 2DRF excitation (26-ms pulse duration, 2-ms gradient rephasing).

The blipped-planar trajectory was further improved by making the distance of the first side excitations (200 mm) an integral multiple of the profile width in the FOV direction (50 mm). Under these circumstances, every fourth line of the trajectory coincided with a zero-crossing of the sinc function. Because no RF power has to be applied for these lines, they can be omitted without affecting the quality of the excitation profile (14). As a result, the 2DRF pulse can be shortened or the gained time can be invested in an improved profile, as chosen here.

The lines sampled by the resulting trajectory (Fig. 1d) cover about 3.5 side lobes of the sinc function along the FOV direction, whereas sampling in the slice direction has been limited to the central lobe extending to the first zero crossing. To reduce ringing artifacts due to truncation, the weighting function was filtered with a 2D Gaussian function (Fig. 1e). An empirical optimization of the filter resulted in a 25% maximum filter strength at the border of the sampled K-space in the slice direction and 15% in the FOV direction. Based on the filtered weighting function (Fig. 1e) the RF field strength $B_1(t)$ was calculated according to Eq. [3]. The resulting simulated excitation profile (Fig. 1f) clearly reveals the blurring of the original profile (Fig. 1a). The profile reflects both the finite K-space sampling and the Gaussian filtering which successfully minimized ringing artifacts. It also demonstrates the prominent side excitations caused by the discrete sampling in the FOV direction.

Experimentally, the developed trajectory (Fig. 1c) consisted of 23 lines through K-space with a total duration of 26.0 ms, i.e., 1.13 ms per line. Apart from the calculated B_1 field, Fig. 2 depicts the corresponding gradient pulse train in the slice direction with a maximum gradient strength of 21.2 mT m^{-1} (530 μs ramp times, 70 μs plateau) and the

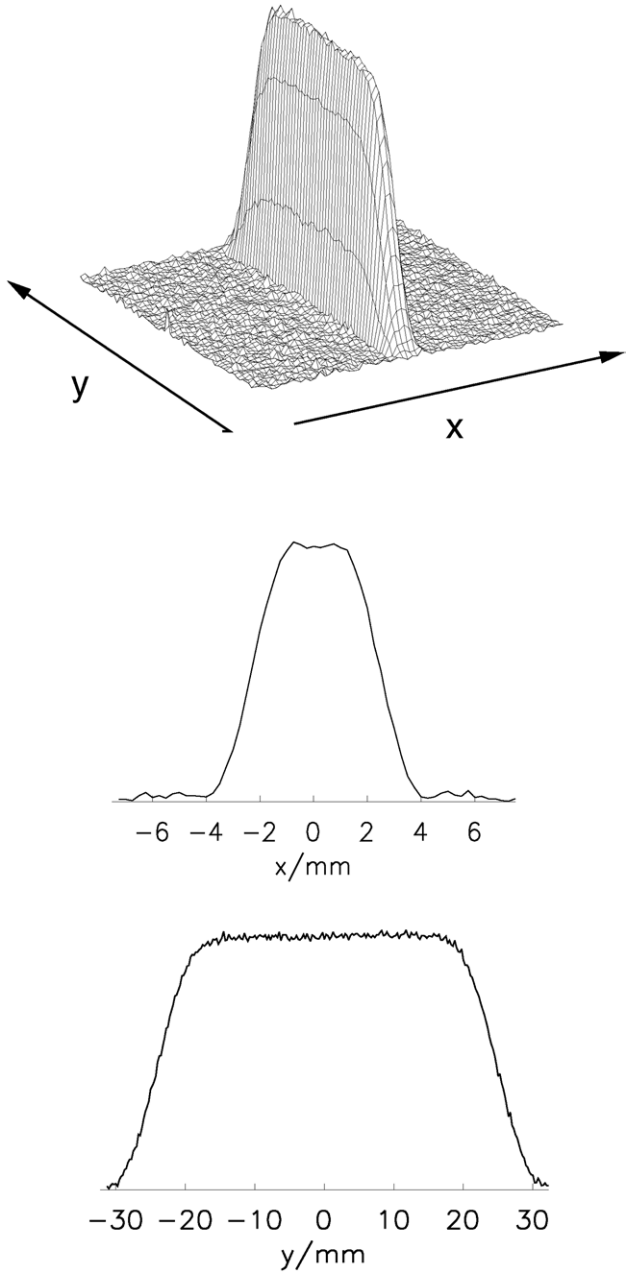

FIG. 3. Experimental excitation profile (5-mm section, 40-mm FOV) of the 2DRF pulse shown in Fig. 2 (fully relaxed spin-echo MRI sequence, TR/TE = 10000/40 ms, water phantom). For details see text.

triangular gradient blips in the FOV direction with a maximum gradient strength of 2.1 mT m^{-1} (120 μs total duration). When omitting lines due to zero-crossings, the necessary "double blips" had a maximum amplitude of 3.1 mT m^{-1} (160 μs total duration).

EPI Sequences With 2DRF Pulses

For single-shot imaging of the human brain with reduced echo-train lengths, 2DRF pulses were incorporated into gradient-echo and spin-echo EPI sequences with a voxel resolution of $2 \times 2 \times 5$ mm^3 based on a 128×128 matrix

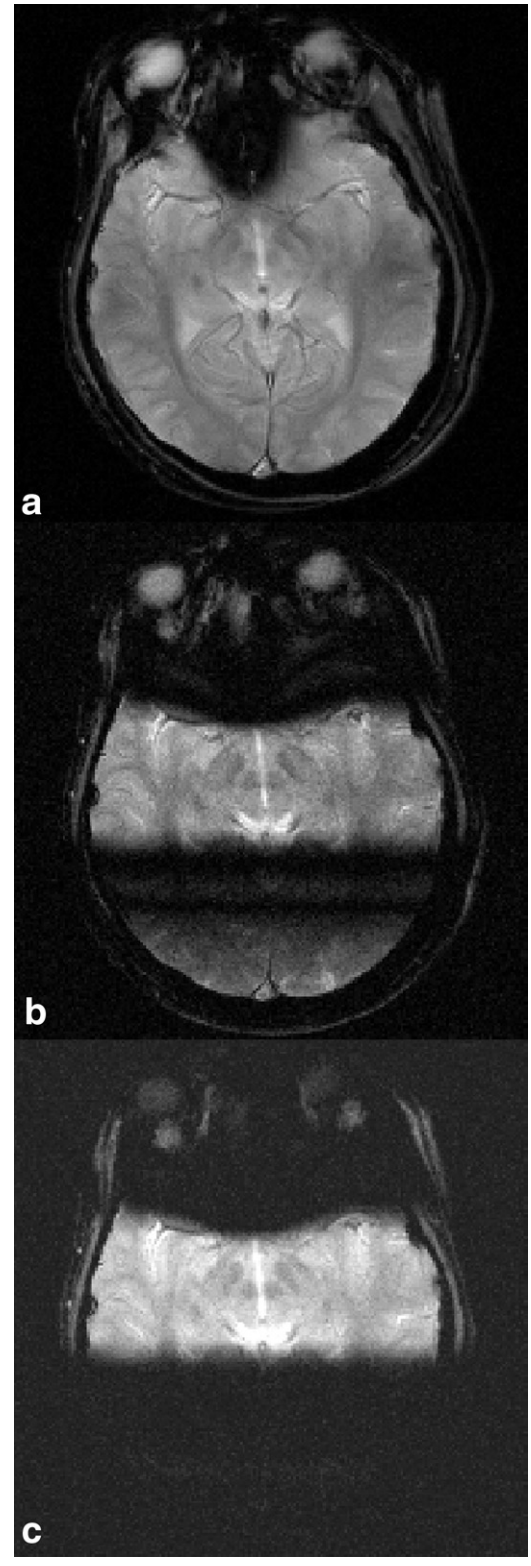

FIG. 4. Reduced FOV imaging (5-mm section, 40-mm FOV) using the 2DRF pulse shown in Figs. 2 and 3 (T_2^*-weighted FLASH, 10° flip angle, TR/TE = 62.5/30 ms, brain of a healthy human subject). (**a**) Conventional RF excitation, (**b**) 2DRF excitation with a 10-μs delay between RF and gradient time courses, and (**c**) 2DRF excitation with optimized timing. For details see text.

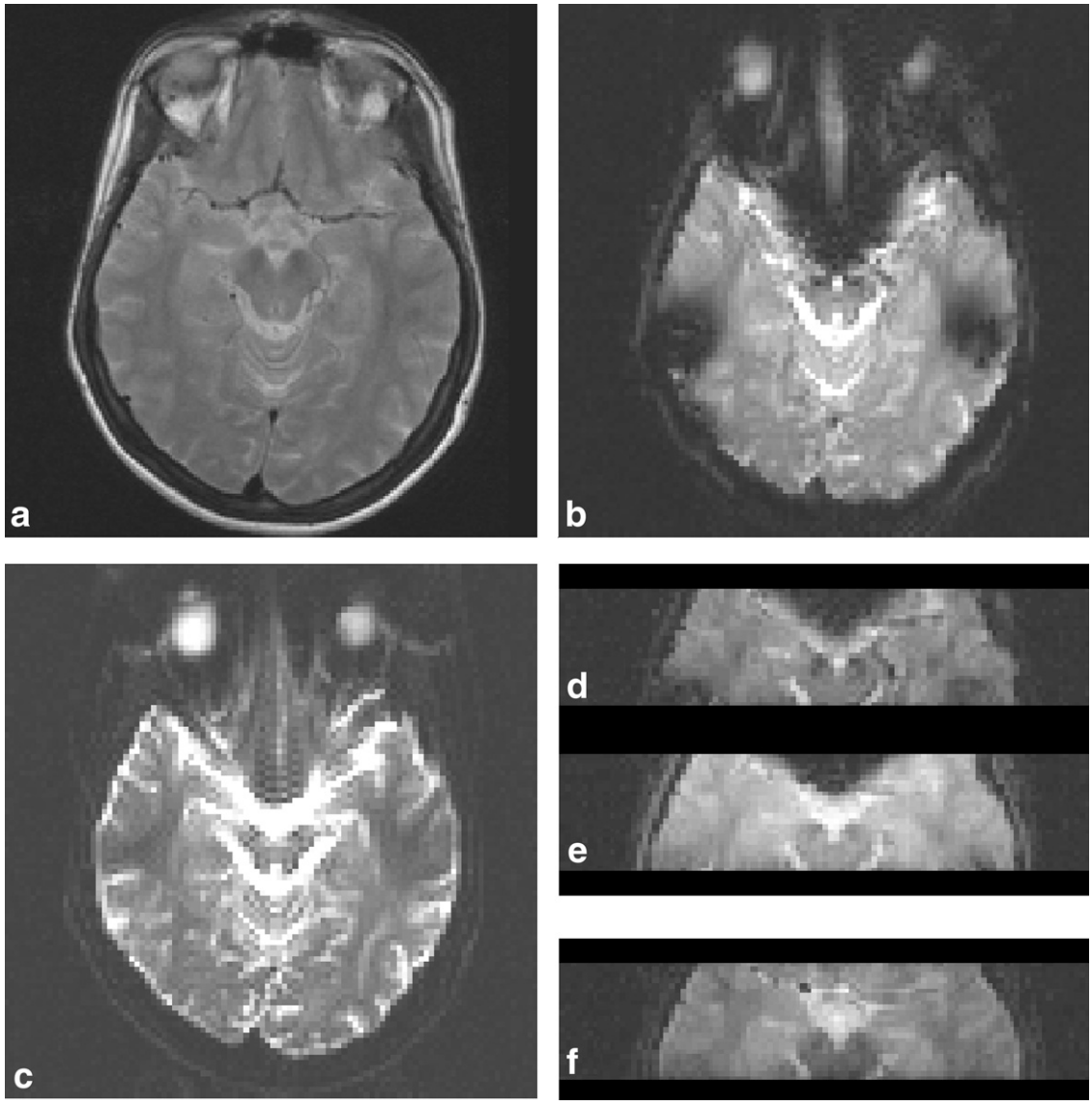

FIG. 5. Susceptibility artifacts in gradient-echo and spin-echo EPI (5-mm section, amygdala of a healthy human subject). (**a**) Anatomical reference (FSE, TR/TE = 2500/98 ms), (**b**) conventional gradient-echo (TE = 59 ms) and (**c**) spin-echo (TE = 121 ms) EPI, (**d**) gradient-echo EPI (TE = 59 ms) with 2DRF excitation (40-mm FOV), (**e**) same as **d** but with minimum TE (30 ms), and (**f**) spin-echo EPI (TE = 60 ms) with 2DRF excitation.

in conjunction with a 256 × 256 mm^2 FOV. For a pixel bandwidth of 1470 Hz and symmetric phase encoding, conventional gradient-echo and spin-echo EPI sequences result in mean echo times (TEs) of 59 ms and 121 ms, respectively. The reduction of the echo train by the 2DRF pulse is proportional to the reduction of the FOV along the phase-encoding direction, in this study from 256 mm to 52 mm (including 12-mm oversampling). The corresponding acquisition of only 26 differently phase-encoded gradient echoes reduced the mean TEs to 30 ms for gradient-echo EPI and 60 ms for spin-echo EPI. In 2DRF-EPI the pixel bandwidth was increased to 1720 Hz to account for the prolonged duration of the phase-encoding blips due to the reduced FOV. To increase the spatial resolution for the small FOV, e.g., to a voxel size of 1 × 1 × 5 mm^3, further modifications generated sequence variants with the acquisition of 52 *k*-space lines and TEs of 50 ms and 104 ms (1020 Hz pixel bandwidth). All spin-echo EPI sequences used a 90° 2DRF excitation pulse in conjunction with a conventional slice-selective 180° refocusing pulse.

RESULTS

Experimental Implementation of 2DRF Pulses

Figure 3 shows the measured excitation volume and respective profiles for the aforementioned 2DRF excitation pulse. These results were obtained with a homogenous water phantom and a conventional, single-echo spin-echo MRI sequence in which the first RF pulse was replaced by a 90° 2DRF pulse perpendicular to the section defined by the 180° refocusing pulse. The excited volume has full

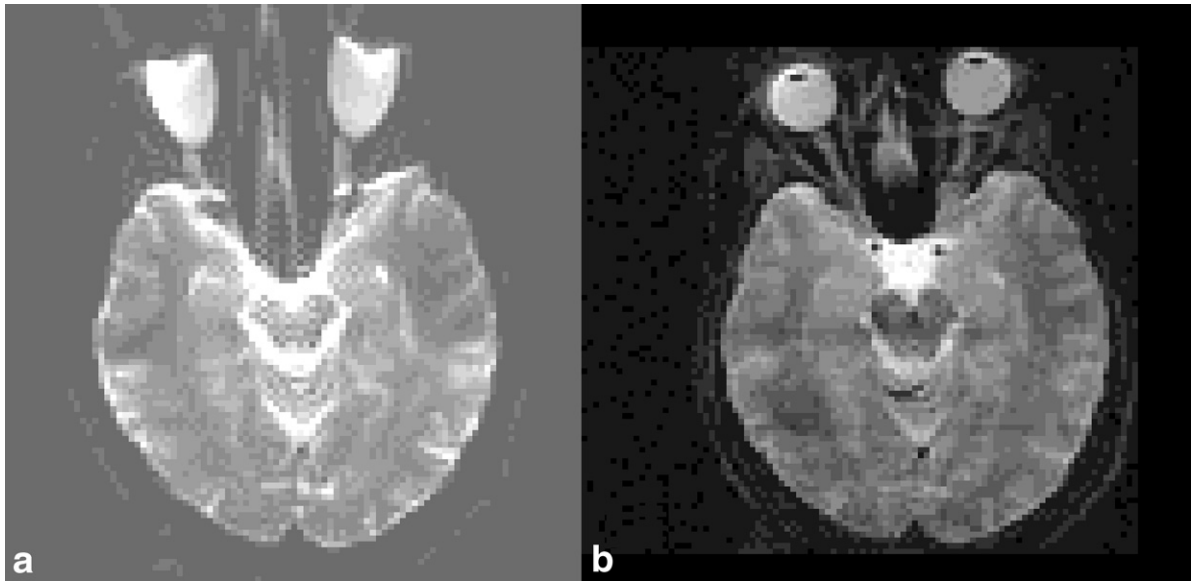

FIG. 6. Spin-echo EPI with 2DRF excitation (5-mm section, amygdala of a healthy human subject). (**a**) Conventional spin-echo EPI (TE = 121 ms) and (**b**) combination of five single-shot images, each obtained by spin-echo EPI (TE = 60 ms) with spatially-shifted 2DRF excitation (40-mm FOV). Because the implemented spin-echo EPI sequence with 2DRF used a slice-selective refocusing RF excitation, the individual images of **b** could not be acquired in rapid succession.

widths at half maximum (FWHM) of 5 × 50 mm^2. The usable FOV is about 40 mm, which corresponds to a plateau with at least 95% of the maximum amplitude.

Cross-sectional images obtained with the 2DRF pulse are shown in Fig. 4 for the case of a fast low-angle shot (FLASH) MRI sequence with T_2^* weighting. They also demonstrate the sensitivity of the blipped-planar trajectory to subtle temporal shifts of the 2DRF field with respect to the gradients. Misadjustments result in a line-by-line alternation of B_1 in K-space, and therefore cause *N/2* "ghost" excitations which appear in between the central volume and the first side excitations (Fig. 4b). Their removal requires a proper setting of the RF and gradient timings (Fig. 4c). Residual signal contributions from outer lipid signals present in the 2DRF-FLASH images are eliminated in fat-suppressed EPI.

EPI With 2DRF Excitation

Figure 5 summarizes single-shot EPI results obtained with either conventional RF excitation or 2DRF pulses. The images represent the same transverse section of the brain of a healthy human subject at the level of the amygdala. In comparison with a fast spin-echo reference image (Fig. 5a), both gradient-echo (Fig. 5b) and spin-echo EPI sequences (Fig. 5c) cause severe geometric distortions and signal losses due to susceptibility-induced magnetic field inhomogeneities in the vicinity of air-filled cavities. Although these artifacts are slightly less pronounced in spin-echo EPI, the images tend to exaggerate the CSF signal because of the long T_2 value. The application of 2DRF pulses considerably improves image quality, at the expense of a reduced FOV and a lower SNR, which results from the decreased number of acquired lines and the slightly increased pixel bandwidth (Fig. 5d–f). As demonstrated for a gradient-echo 2DRF-EPI sequence, susceptibility artifacts are reduced because of both the reduction of the echo-train length at the same mean TE (Fig. 5d) and the additional possibility of decreasing the TE to 30 ms (Fig. 5e). In the latter case, and in contrast to conventional gradient-echo EPI, the image shows almost no distortions in the amygdala region, while retaining a TE that provides sufficient T_2^* contrast for the detection of deoxyhemoglobin-based MRI signal changes in response to neuronal activation. Functional neuroimaging in critical brain regions may therefore become a potential target for gradient-echo 2DRF-EPI.

In terms of image quality, the results for spin-echo 2DRF-EPI are even more promising (Fig. 5f), as both geometric distortions and signal losses become almost invisible. Figure 6 demonstrates that this holds true even for regions that are severely affected by structural inhomogeneity artifacts such as the eyes and the optic nerve. Rather than measuring a conventional image by single-shot EPI and a mean TE of 121 ms (Fig. 6a), a distortion-free image of the full FOV may be obtained by the summation of multiple spatially-shifted single-shot images at reduced FOV obtained with spin-echo 2DRF-EPI at TE = 60 ms (Fig. 6b).

The reduced echo-train length for 2DRF-EPI offers access to higher spatial resolution, which is normally precluded because of the need for additional phase-encoded gradient echoes. An example of high-resolution spin-echo 2DRF-EPI of the human brain is demonstrated in Fig. 7. The use of a conventional spin-echo EPI sequence at 2 × 2 mm^2 resolution and TE = 121 ms results in considerable blurring of the cerebellar gyration (Fig. 7a and b). Markedly improved structural delineations are obtained with spin-echo 2DRF-EPI at 1 × 2 mm^2 (Fig. 7c) or even 1 ×

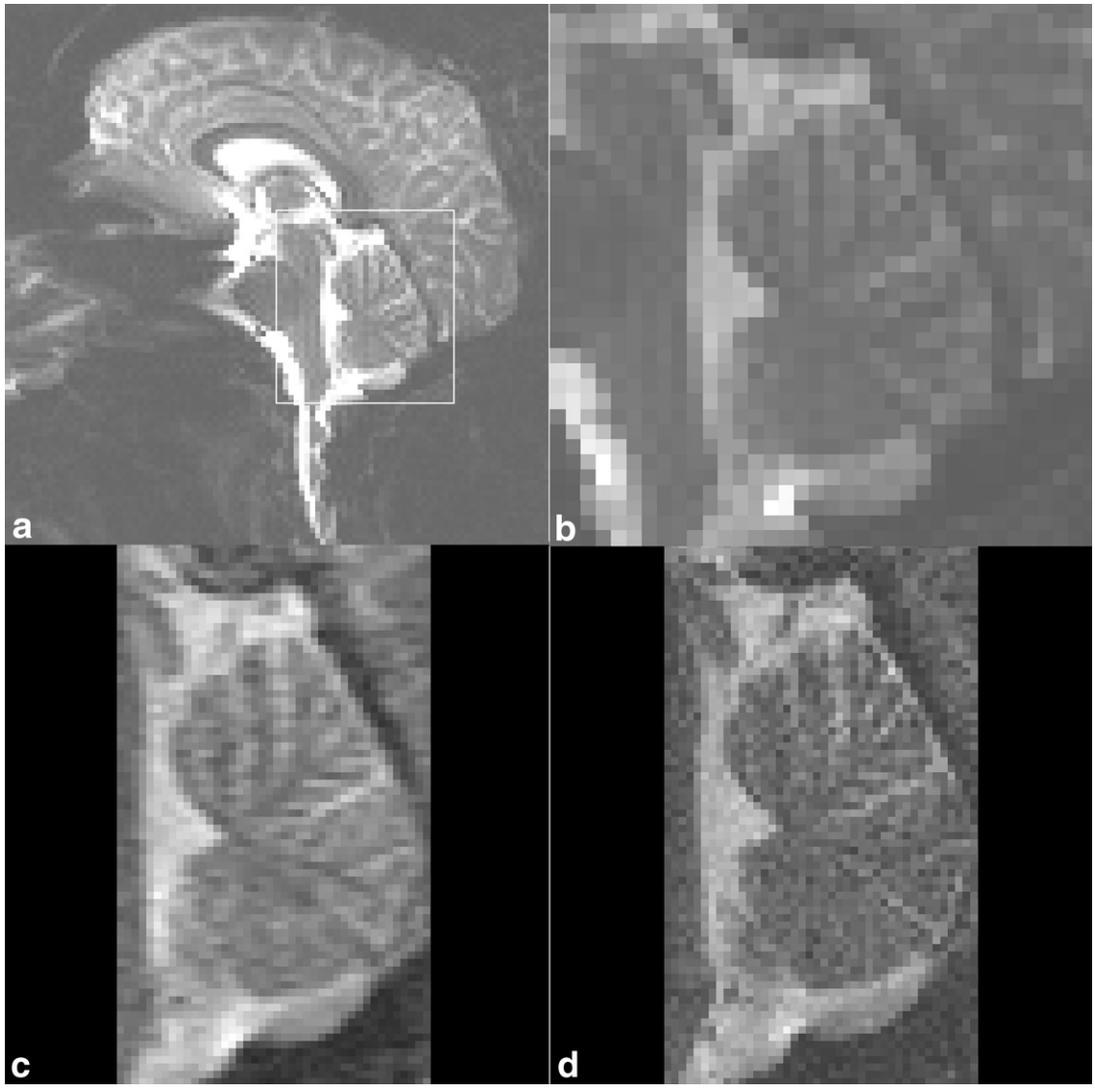

FIG. 7. High spatial resolution in spin-echo EPI with 2DRF excitation (5-mm section, 40-mm FOV, cerebellum of a healthy human subject). (**a**) Conventional spin-echo EPI (TE = 121 ms) at 2 × 2 mm^2 resolution, (**b**) magnified view of the area indicated in **a**, (**c**) spin-echo EPI with 2DRF excitation at 1 × 2 mm^2 resolution (TE = 72 ms), and (**d**) at 1 × 1 mm^2 resolution (TE = 104 ms).

1 mm^2 resolution (Fig. 7d). It is noteworthy that the latter images are at much shorter TEs (72 ms and 104 ms) than obtained for conventional EPI at identical resolution.

DISCUSSION

The present work demonstrates the design and experimental application of 2DRF pulses for single-shot EPI of the human brain. The technique bears considerable potential for overcoming some of the inherent limitations of conventional EPI techniques. In particular, for a reduced FOV, 2DRF-EPI sequences allow for improved image quality in terms of markedly reduced susceptibility artifacts, and provide access to higher spatial resolution. These sequences may contribute to more reliable studies of brain regions close to major air cavities, especially in view of the need for counteracting the much more pronounced susceptibility problems in high-field MRI systems at 3.0 T and beyond. Specific applications are likely to emerge for functional neuroimaging and diffusion-weighted imaging exploiting gradient-echo and spin-echo variants of single-shot 2DRF-EPI, respectively.

The physical reason for the low sensitivity to resonance offset effects is the much shorter train of phase-encoded gradient echoes that is required when covering only a small FOV. The beneficial effect to the actual image stems from both the shorter echo train (at a given TE) and the possible reduction of the mean TE. On the other hand, the improved image quality is at the expense of a smaller FOV and a lower SNR due to the decreased number of acquired gradient-echo signals. If the coverage of a large FOV is desired, several images of spatially shifted FOVs may be combined. Because this "segmentation" is performed in image space using magnitude images, the procedure is insensitive to phase variations between complex MRI signals from different image segments. For gradient-echo

2DRF-EPI, the absence of spatial presaturation outside the imaging volume allows for successive acquisitions of individual single-shot image segments without any repetition delay. The residual in-plane overlap originating from oversampling of the excitation profile along the phase-encoding direction may be circumvented by interleaved acquisitions, as commonly used for multislice imaging. In spin-echo 2DRF-EPI the problem of in-plane saturation due to the slice-selective refocusing RF pulse applied here can be avoided by also using a 2DRF refocusing pulse. However, the design of a 180° 2DRF refocusing pulse should be based on more sophisticated theoretical approaches extending the low flip approximation, as suggested in Ref. 18.

The 2DRF pulse developed here represents a close to "worst case" scenario. For many applications, less stringent boundary conditions are possible which either shorten the duration of the 2DRF pulse or improve its performance. For example, for functional neuroimaging of the amygdala or diffusion-weighted MRI of the spine, the distance of the FOV to the side excitations may be reduced to 150 mm, which translates into a 2DRF pulse duration of only 17 ms (15 K-lines) rather than 26 ms. Moreover, the use of the maximum available gradient slew rate would further decrease the pulse duration to 12.8 ms, i.e., 0.75 ms per K-line. Obviously, the saved time of about 13 ms may be used for a shorter TE or converted into a better and thinner section profile. On the other hand, pulse durations longer than 26 ms might be suitable for spin-echo 2DRF-EPI because a longer TE does not enhance image artifacts. Furthermore, it may be worth considering other K-space trajectories to overcome limitations caused by N/2 excitations. For sagittal or coronal image orientations, the circular side excitations of a spiral trajectory may be shifted outside the head, unlike in transverse orientations where they cross the neck. Off-resonance effects during the 2DRF excitation mainly result in a spatial shift of the excitation profile in the FOV direction. For the current implementation using the blipped-planar trajectory, a change of the transmitter frequency of 100 Hz would cause a spatial shift of 22 mm without affecting the slice profile.

Finally, a remaining (though temporary) problem is that the 2DRF pulses are difficult to implement because no automatic procedure for pulse calculations and routine is currently available on commercial MRI systems. Nevertheless, 2DRF pulses are likely to become a useful addition to the arsenal of advanced MRI tools.

ACKNOWLEDGMENTS

The authors thank Thomas Kluge and Siemens Medical Systems for the algorithm used to calculate the 2DRF waveforms.

REFERENCES

1. Mansfield P. Multi-planar image formation using NMR spin echoes. J Phys C 1977;10:55–58.
2. Ahn CB, Kim JH, Cho ZH. High-speed spiral-scan echo planar NMR imaging. IEEE Trans Med Imaging 1986;5:2–7.
3. Cho ZH, Ahn CB, Kim JH, Lee YE, Mun CW. Phase error corrected interlaced echo planar imaging. In: Proceedings of the 6th Annual Meeting of SMRM, New York, 1987. p 912.
4. McKinnon GC. Ultrafast interleaved gradient-echo-planar imaging on a standard scanner. Magn Reson Med 1993;30:609–616.
5. Sodickson DK, Manning WJ. Simultaneous acquisition of spatial harmonics (SMASH): fast imaging with radiofrequency coil arrays. Magn Reson Med 1997;38:591–603.
6. Pruessmann KP, Weiger M, Scheidegger MB, Boesiger P. SENSE: sensitivity encoding for fast MRI. Magn Reson Med 1999:42:952–962.
7. Griswold MA, Jakob PM, Nittka M, Goldfarb JW, Haase A. Partially parallel imaging with localized sensitivities (PILS). Magn Reson Med 2000;44:602–609.
8. Bammer R, Stollberger R, Hartung HP, Fazekas F. Parallel imaging strategies for reduction of resonance offset induced artifacts and k-space filtering effects. In: Proceedings of the 8th Annual Meeting of ISMRM, Denver, 2000. p 1503.
9. Mansfield P, Ordidge RJ, Coxon R. Zonally magnified EPI in real time by NMR. J Phys E 1988;21:275–280.
10. Turner R, von Kienlin M, Moonen CTW, van Zijl PCM. Single-shot localized echo-planar imaging (STEAM-EPI) at 4.7 T. Magn Reson Med 1990;14:401–408.
11. Yang GZ, Gatehouse PD, Keegan J, Mohiaddin RH, Firmin DN. Three-dimensional coronary MR angiography using zonal echo planar imaging. Magn Reson Med 1998;39:833–842.
12. Pauly JM, Nishimura D, Makovski A. A k-space analysis of small-tip-angle excitation. J Magn Reson 1989;81:43–46.
13. Pearlman JD, Hardy CJ, Cline HE. Continual NMR cardiography without gating: M-mode MR imaging. Radiology 1990;175:369–373.
14. Alley T, Pauly J, Sommer F, Pelc N. Angiographic imaging with 2DRF-pulses. Magn Reson Med 1997;37:260–267.
15. Börnert P, Schäffter T. Curved slice imaging. Magn Reson Med 1996; 36:932–939.
16. Finsterbusch J, Frahm J. Gradient-echo line scan imaging using 2D-selective RF excitation. J Magn Reson 2000;147:17–25.
17. Kluge T. Zweidimensional ortsselektive Anregung eines Spinensembles mit einem kommerziellen Kernspintomographen. Diploma thesis, University of Bayreuth, 1997.
18. Pauly JM, Spielman D, Macovski A. Echo-planar spin-echo and inversion pulses. Magn Reson Med 1993;29:776–782.